Peptides as Biosorbents - Promising tools for resource recovery

Braun, R.; Bachmann, S.; Schönberger, N.; Matys, S.; Lederer, F.; Pollmann, K.;

Originally published:

June 2018

Research in Microbiology 169(2018)10, 649-658

DOI: https://doi.org/10.1016/j.resmic.2018.06.001

Perma-Link to Publication Repository of HZDR:

https://www.hzdr.de/publications/Publ-27183

Peptides as Biosorbents – Expanding the toolbox for Resource Recovery

Robert Braun[a*], Stefanie Bachmann[a], Nora Schönberger[b], Sabine Matys[a], Franziska Lederer[a], Katrin Pollmann[a]

[a]Helmholtz-Zentrum Dresden-Rossendorf, Helmholtz Institute Freiberg for Resource Technology, 01328 Dresden, Germany

[b]Technische Universität Bergakademie Freiberg, Institute of Non-Metallurgy and Pure Substances, 09599 Freiberg, Germany

r.braun@hzdr.de *Correspondence and reprint, s.bachmann@hzdr.de, n.schoenberger@hzdr.dr, s.matys@hzdr.de, f.lederer@hzdr.de, k.pollmann@hzdr.de

Abstract.

Despite many innovations, meeting both economic and ecological requirements remains challenging for conventional resource recovery technology. The development of highly selective peptides puts a new competitor on the market. We present an approach to identify peptides for resource recovery using Phage Surface Display. Here, we describe the development of peptides for binding of rare earth element terbium-containing solids and for removal and enrichment of the heavy metal ions of cobalt and nickel out of waste waters and leaching solutions.

Keywords: phage display; biosorption; peptide; biohydrometallurgy

Introduction.

Usage of biology in mining was first commercially applied in the 1950s, when the exploitation of bacteria for copper extraction was patented. Since then dump bioleaching is the fundamental part for the extraction of valuables from marginal-grade ore. Heap bioleaching and stirred-tank bioextraction were utilized commercially beginning in the 1980s [1]. The increasing importance of biomining regarding the growing usage of bacteria and described reaction principles were comprehensively reviewed by Bosecker (1997) [2] and Johnson [3,4]. Even extraction of valuables from non-mineral resources as metallic wastes are nowadays being discussed. For most processes and bacteria used, even the molecular pathways are very well described and the intra-bacterial mechanism are known in detail [5]. However, up to now, biomining only covered the usage of bacteria. Bacteria are complex living constructs with constant need for substrates, changing demands and reactions depending on the conditions used for metal recovery. Interaction of metals and bacteria is mostly accomplished by different proteins and enzymes, such as cytochromes [6], with redox pathways typically used for bioleaching only contributing a small part to the complete metabolism. Unlike in bioleaching, where binding of target elements and redox transformations are equally important, in biosorption binding of target substances is of main importance. As a result, systems using chemicals with functionalities borrowed from nature are already being applied for bioflotation or e.g. flocculation. Therefore, the potential use of a proteinic biological system, which only provides metal binding capacity would benefit from leaving behind other biological fluctuations. It also becomes more attractive, as peptides and proteins usually show high sensitivity and selectivity towards their target molecules. For most biohydrometallurgical purposes acidification is also necessary, which is wasteful and not required anymore when only the metal-binding proteins are being used. Other biological molecular systems using complexing molecules, which are available for biosorption are e.g. siderophores [7].

In this study, we describe how to select und utilize only the protein domains, which are obligatory for metal-interaction using Phage Surface Display (PSD). In the last decades PSD has mainly been used in medical context such as the discovery of diagnostic and therapeutic peptides e.g. for the recognition of cancer. However growing interest is nowadays drawn to the identification of inorganic binding peptides [8], e.g. hydroxyapatite for medical devices. Phage Surface Display uses the unique characteristic of phage, the combination of genotype (DNA encoding the phage structure) and phenotype (the proteinic structure of the phage) without the influences of living nature. Every living cell possesses a metabolism. It is

subjected to a constantly changing environment resulting in a constantly changing structure of the cells. Phage however, can be considered as a molecular building block as they show no metabolism and variability of structure. For PSD, a DNA sequence coding for a short peptide motif, is added to DNA sequence of the coat proteins of the phage, resulting in phage displaying these short peptide motifs. Libraries of phage can be created that include billions of different sequence motifs, which can be used for the identification of target-specific peptides.

Recently, usability of PSD for solid- and inorganic material binding was shown and is well summarized in the reviews of Seker & Demir (2011) and Care et al. (2015) [9,10]. However, application areas were mainly described in medicine and nanotechnology, e.g. for biosensors and biomaterials. With this work, we expand the usability of PSD and the boundaries of biomining by identification and characterization of peptides that are binding to metal ions from waste waters and leachates as well as binding to solids, e.g. from solid scrap for the recovery of rare earth element (REE)-containing compounds as shown in Fig. 1. Perspectively, these peptides can be addressed to genetic engineering for adaption and modification, e.g. for immobilization and reusability or to simplify heterologous production.

Materials and methods.

Phage libraries and bacterial strains. Experiments for the identification of terbium-binding peptides were performed using the LX-4 library, a random PVIII phage library, kindly provided by Dr. Jamie Scott (Simon Fraser University, Burnaby, BC) [11]. Selection of phage and peptide sequences able to bind to nickel or cobalt was performed with the Ph.D.^{TM}-C7C phage library (NEB, US), displaying randomized peptides on the PIII coat protein. All displayed peptides possess the amino acid sequence ACXCGGG, with X being a motif of seven randomized amino acids. The bacterial strain used for phage amplification was *E. coli* ER2738 (F' *proA*$^{+}$*B*$^{+}$ *lacI*^{q} *Δ(lacZ)M15 zzf::Tn10(Tet*^{R}*)/fhuA2 glnV Δ(lac-proAB) thi-1 Δ(hsdS-mcrB)5*).

Phage Surface Display for solid-binding peptides. Terbium doped cerium-magnesium aluminate (CAT) (Leuchtstoffe Breitungen GmbH, Germany), an indispensable part of fluorescent powder of compact light bulbs, was used for the selection of specific binding peptides out of recombinant phage library. Experiments were performed as described elsewhere [12,13]. The main steps are summarized below, for detailed descriptions please refer to Lederer et al. (2017). Samples of CAT were washed and subsequently blocked with Tween 20 and BSA. After extensive washing ~ 2×10^{11} phage particles displaying 1.5×10^{9} different randomized peptides were incubated with the pretreated mineral. Removal of weakly bound phage was achieved by subsequent repeated washing. Elution of strong binding phage was carried out by lowering the pH or alternatively achieved by incubating the material directly with freshly prepared *E. coli* cells. Amplification of phage was achieved by infection of freshly prepared *Escherichia coli* K91 [14]. Infected cells were cultivated and induced with IPTG. Isolation of produced phage particles was performed via PEG precipitation as described elsewhere [14]. Enrichment of specific binding phage usually requires several rounds of biopanning with enhanced stringency to select strongly binding phage. Therefore, three rounds of biopanning were performed with increasing concentration of Tween 20 in binding and washing buffer. After completion of three rounds of biopanning, phage containing supernatant of colonies of infected *E. coli* cells was used as template for PCR amplification.

Phage Surface Display for ion-binding peptides. The biopanning selection process of phage for ion specific binding has been accomplished using planar sol gel materials (GMBU e.V., Germany) with ion exchange properties. Experiments and preparations were carried out as described by Schönberger et al. 2017 [15]. Sol gel materials were prepared with cationic

binding capacity using tetraethylorthosilicate (TEOS) and different polymers (15 % w/w Dispex N40, polyacrylic acid or polystyrene sulfonate). For biopanning the sol gel materials were loaded with divalent nickel or cobalt-salt containing buffers. Preparation, binding procedure, washing steps and elution were performed as described by Schönberger et al. Selection pressure in the different biopanning rounds was accomplished by lowering the pH. Elution was alternatively achieved by incubating the material directly with freshly prepared *E. coli* ER2738 cells. Amplification of phage was performed as described elsewhere [14]. After determination of phage concentration, the supernatant of the phage containing, infected colonies of *E. coli* cells was used as template for PCR amplification.

Sequencing. Sanger sequencing was carried out by GATC Biotech AG (Germany). For the LX-4 phage library oligonucleotide primers were: (forward) 5'-GCTCTAAATCGGGGGAGCT-3'; (reverse) 5'-CATAAGCTAGCTTAAAAAAAAGCCCGC-3'. For Ph.D.^{TM}-C7C phage libraries oligonucleotide primers were: (forward) 5'-GCAACTATCGGTATCAAGCT-3'; (reverse) 5'-CCCTCATAGTTAGCGTAACG-3'. Amplified PCR products were used for sequencing and identification of recombinant peptide sequences. The primer sequences used for Sanger sequencing were 5'-CCCTCATAGTTAGCGTAACG-3' (C7C) and 5'-AGTAGCAGAAGCCT- GAAGA-3' (LX-4).

Binding Assay for solid-binding peptides. Pre-identified phage, derived from single clone amplification out of colonies of infected cells, were characterized concerning their ability to bind to individual components of fluorescent lamp powder and to quantify the selective binding behavior. Components tested were $CeMgAl_{11}O_{19}:Tb^{3+}$ (CAT), $Y_2O_3:Eu^{3+}$ (YOX), $BaMgAl_{10}O_{17}:Eu^{2+}$ (BAM), $LaPO_4$:Ce,Tb (LAP) and halophosphate (HP). Mineral preparation, phage production and binding studies were performed as described elsewhere [12]. Mineral dispersions were incubated together with the phage and subsequently repeatedly washed, resulting in the removal of weakly bound phage. Phage concentrations in input and eluate were determined and compared to the binding behavior of wild-type fd-tet phage (obtained by Dr. Jamie Scott). Calculated values describe the ratio of bound phage in eluate compared to phage input concentration normalized against the wild-type phage values. The binding assay for cobalt and nickel-binding phage was conducted as described here, however nitrilotriacetic acid (NTA) sepharose with either immobilized nickel or cobalt was used as binding material. Same buffers as in the preceding biopanning experiments were used.

Competitive Binding. Competitive binding characterization was done using defined phage libraries of amplified phage. Libraries were created by using equimolar concentrations of phage (1×10^{10} Pfu mL^{-1}), which have previously been identified in the biopanning process. The method was performed as described earlier [12,16].

Immunofluorescence. Fluorescence microscopy (Olympus; Japan). was used to compare the intensity of emitted fluorescence of minerals and phage, which were treated with fluorophore-labeled antibodies. Phage were firstly marked with a primary, phage-binding antibody, which was subsequently treated with a secondary fluorophore-labeled antibody, specifically binding the primary antibody. Preparation of CAT mineral, phage binding, washing and sample preparation for microscopy were performed as described by Lederer et al. (2017) [12].

Results.

Solid-binding peptides. Random peptide sequences with high affinity to CAT minerals were identified from the PVIII phage library LX-4. After three rounds of biopanning corresponding DNA sequences of the displayed peptides on phage of 80 infected colonies were amplified via PCR and sequenced. 11 different sequences were determined which generally showed a high content of amino acids with charged side-chains, especially lysine. KKQKCRTDACVTQM was the most-occurring sequence and was found 7 times, other sequences were found only with lower frequency. Table 1 shows a list of all identified sequences and the general composition of their amino acid sequences. All identified peptides possess a high proportion of charged, hydrophilic amino acids while hydrophobic and acidic amino acids are absent or occur in low frequency. For further characterization of the binding affinity of the peptides to CAT minerals, a competitive binding assay was carried out. 30 colonies of infected bacteria were characterized in regards of the displayed peptide sequence. Results can be found in Table 1. Interestingly the monitored sequence frequencies strongly differ from the relative occurrence of peptides after panning with the original library. Peptides, which were originally found in smaller proportions now contribute to nearly half of all identified sequences. Most of the identified peptide sequences resemble in their theoretical isoelectric point being above 8.8 resulting in a positive net electrical charge at pH 7.5, which was chosen for biopanning. The most frequent sequences KKQKCRTDACVTQM (SB1), NEKKCKGARCTTVT (SB2), ATPKCKKKSCMTTQ (SB3) and ETKKCTTGPCKVVT (SB4) were chosen for further binding assays.

Binding of amplified phage as ratio of phage input titer and phage elution titer was determined with CAT minerals for at least three times. Results are shown in Fig. 2. All tested phage had a higher binding efficiency against the tested materials as wild-type phage, indicating that preceded biopanning had successfully selected peptide sequences with high affinity to CAT. Measured binding efficiencies of sequences NEKKCKGARCTTVT (SB2 84.3 ± 19.4), ATPKCKKKSCMTTQ (SB3 94.5 ± 29.9) and KKQKCRTDACVTQM (SB1 128.6 ± 23.5) were in a similar range, while binding efficiency of ETKKCTTGPCKVVT (SB4 13.4 ± 4.7) was only slightly increased in comparison to the wild-type binding properties. Although being dominant in the competitive occurrence measurements, the binding efficiency was more similar to the wild-type phage than to the other identified sequences.

Immunofluorescence labeling was performed to visualize the binding and to describe the distribution of bound phage, as shown in Fig. 3. Phage SB1 displaying the peptide KKQKCRTDACVTQM and wild-type phage were incubated with CAT and marked with the antibodies. CAT mineral is showing autofluorescence at 360 – 410 nm (filter U-MNU), however with filter U-N39010 (540 – 580 nm) fluorescence of the secondary antibody can be visualized. In Fig. 3 phase contrast and fluorescence microscopy pictures using different filters are shown. CAT minerals used had a size of 5 – 15 µm. Visualization of phage was possible with filter U-N39010 showing high fluorescence in picture B3 which is somewhat reduced after elution (compare B6). Only weak fluorescence was detected for CAT mineral treated with wild-type phage, which further decreased after the elution. Similar effects were seen for Phage SB2, SB3 and SB4 (results not shown).

Besides the binding ability to CAT, peptides for future industrial purposes may need to discriminate between different materials. Therefore binding studies with $CeMgAl_{11}O_{19}:Tb^{3+}$ (CAT), $Y_2O_3:Eu^{3+}$ (YOX), $BaMgAl_{10}O_{17}:Eu^{2+}$ (BAM), $LaPO_4:Ce^{3+},Tb^{3+}$ (LAP) and halophosphate (HP) were conducted, materials typically found in fluorescent lamp powder. Results are shown in Fig. 4. Binding efficiency was calculated using phage titer before and after binding assays in comparison to the wild-type phage. Peptide sequences used for comparison were KKQKCRTDACVTQM, NEKKCKGARCTTVT, ATPKCKKKSCMTTQ and ETKKCTTGPCKVVT, which were predominantly identified either in original biopanning experiments or in subsequent competitive binding experiments using mini libraries.

Binding behavior towards different materials differs between the tested phage. All tested sequences show a higher affinity towards CAT compared to wild-type phage (compare Table 1). While the binding affinity towards LAP and BAM of SB1 is equally high as for CAT (LAP 126 ± 6, BAM 148 ± 7, CAT 128 ± 23), both SB2 and SB3 show a specific binding affinity towards CAT, which is ~ 3 times higher as the normalized binding efficiency towards LAP and BAM. However, it has to be highlighted, that binding efficiencies for both materials and peptide sequences are strongly increased compared to the wild-type binding behavior (SB2: LAP 28 ± 3, BAM 29 ± 6; SB3: LAP 31 ± 0, BAM 39 ± 2). Binding affinities for SB4, which showed dominant occurrence in competitive binding assays, follow another trend. While the peptide sequence does only show a slight increase in binding efficiency towards CAT (13 ± 5) and LAP (4 ± 2), affinity for BAM is drastically increased compared to the wild-type phage (58 ± 37). All tested phage possessed affinities to YOX and halophosphate, which are comparable with the wild-type phage behavior. Consequently, only

phage displaying the sequences SB2 and SB3 can be considered as selective for CAT in the range of tested materials. While SB1 shows equally good binding affinities for CAT, LAP and BAM, SB4 even shows a higher affinity to BAM compared to CAT.

Ion-binding peptides. Metal ions such as cobalt(II) and nickel(II) ions were chosen as another target for phage selection. Peptides specifically binding these ions are attractive bioligands for the construction of biosorptive materials. Biopanning was carried out on planar sol-gel surfaces. Sol-gels with cation exchange properties were fabricated using Dispex N40, polyacrylic acid or polystyrene sulfonate, as described elsewhere [17]. Selection pressure for peptide identification was achieved using lowered pH values over the biopanning rounds. In Table 2 all identified peptide sequences as well as their frequencies are shown. The theoretical pI of the peptide, calculated with Expasy ProtParam [18] and the general amino acid composition are shown because the net charge of the peptide and properties of amino acid side chains have a high impact on the binding behavior. In the biopanning experiments that were performed in order to identify cobalt (II)-binding peptides, 63 colonies were examined for their peptide sequence. 28 unique sequences were identified, whereof 22 sequences occurred only once. The peptides sequence MSTGLSS (SMC01) occurred 28 times, constituting nearly half of all analyzed sequences. Further the sequence VPILEGT (SMC02) was identified 5 times, and the peptides DRTISNK (SMC03), QNPGNTL (SMC04), SGTGASY (SMC05) and SSSVVTH (SMC06) were found with each two times. Especially the more frequent sequences except DRTISNK (SMC03) possess a low theoretical pI around 4 – 5.5. All sequences also have a relatively high content of hydroxylic and polar amino acids, while charged amino acids are only found in smaller numbers and aromatic amino acids are nearly absent. Especially in case of sequences that are found only once, the theoretical pI shows a clear difference to more abundant sequences, having values of 8 or higher. In comparison, sequences that were identified to bind to nickel (II) ions generally show a more equal distribution. 29 colonies were sequenced and 24 unique peptide sequences were identified. Only SGTGASY (SMN01) occurred 3 times, whereas MSTGLSS (SMN02), NTGSPYE (SMN03) and TASQNFY (SMN04) each were identified two times. The general properties of the identified nickel-binding peptides are similar to the cobalt-binding peptides. In particular, the peptides have high contents of hydroxylic and polar amino acids whereas charged amino acids occur only in minor amounts and aromatic amino acids are nearly absent. Especially peptide motifs with a higher frequency show a relatively low theoretical pI of about 5, while the other sequences possess pI values typically > 8 but within a range of 4 – 11.

The binding properties of the identified peptide motifs were determined by performing binding assays comparing phage input titer and phage titer in elution fractions after extensive washing. Measured values were normalized against the binding behavior of wild-type phage. Results are graphically shown in Fig. 5 A and are listed in detail in Table 2. Binding experiments were performed only for the most promising sequence motifs. As shown in Fig. 5A the normalized binding efficiencies of nickel-binding motifs were 18 times higher compared to the wild-type. Interestingly two motifs with the strongest binding efficiency towards nickel (SMN06, SMN12) both occurred in the biopanning with a frequency of 01/29 and possess a pI above 8. The three peptide motifs SMN4, SMN01, SMN02, occupying the second place in terms of binding affinity, were found with a frequency of 02/29 in the preceding biopanning. All three peptides possess a pI of about 5. In addition, many sequence motifs were identified that show a binding behavior comparable to the wild-type even after three rounds of biopanning with increased selection pressure. Distribution of cobalt-binding peptide motifs was more uniform as shown in Fig. 5 B. Identified sequences showed a binding efficiency with 0.8 – 3.1 times higher than the wild-type. Sequences occurring with higher frequency generally showed a stronger binding affinity (compare SMC01, SMC04, SMC06). However, the strongest binding peptide motif SMC28 was found only once in the preceding biopanning. Stronger binding sequences tended to possess a theoretical pI of about 5.

As peptides for resource recovery need to be sensitive and selective, promising candidate motifs were used for further binding assays. Peptides, which were originally identified as nickel-binding sequences, were characterized for their binding efficiency towards cobalt and vice versa. In Fig. 6 selected sequences are compared regarding their binding affinities. Besides the normalized binding efficiency, the ratios of efficiencies for nickel and for cobalt are displayed. Some sequences (e.g. SMC15) bound nickel and cobalt in similar amounts, even if they were identified only in the biopanning for one of the heavy metal ions. Interestingly, the affinity of e.g. SMC17, which was selected as cobalt-binding peptide, to nickel is even higher. In contrast, SMC12 that was selected as cobalt-binding peptide, shows a high affinity for cobalt and a lower affinity to nickel.

Discussion.

Solid-binding peptides. Peptide sequences with a high affinity towards CAT mineral were identified from the PVIII phage library LX-4. Frequency of the identified phage differed from 01/80 to 07/80. Sequences chosen for further experiments had a frequency of at least 03/80 with the exception of SB4. This motif showed an initial frequency of 01/80 in the original biopanning but its occurrence in competitive binding assays drastically increased to 14/30, being the most abundant sequence in this assay. pI of all identified motifs was found to be above 8.8 with the exception of VDKKCKSDDCGAWH (theoretical pI 6.7). All sequences showed a high content of hydrophilic and basic amino acids. Acidic and hydrophobic amino acids were only found in small numbers with aromatic amino acids being nearly absent, although acidic amino acids were highly over-represented in peptides discovered by Ploss et al. to bind to metallic borides [16]. A high content of polar amino acids is consistent for all identified motifs. Especially the charged side-chains indicate a surface charge of the CAT minerals used for biopanning. As described by Curtis et al. [13], charged and polar amino acids interact with REE material. The basic amino acid mainly found was lysine (K) with no identified sequence containing less than three lysine. As the pK of the ε-amino group is at 10.28, it shows a positive charge at pH 7.5 chosen for biopanning. However, pK ~ 6.0 of the imidazole side chain of histidine results in a negative charge of the amino acid at pH 7.5. Low occurrence of acidic amino acids may be due to the chosen experimental setup with the pH strongly affect the properties of these side-chains. One underlying mechanism may be electrostatic interaction, as shown by Hatanaka for peptide interaction with charged REE [19]. Chen showed, that the binding mechanism of several metal oxides was of electrostatic nature [20]. Also, Rosi and Chen described electrostatic interaction to be the main interaction principle between inorganic materials and peptides besides complexation by protein folding [21].

Affinity towards CAT mineral was determined for peptide sequences SB1, SB2, SB3 and SB4 which occurred predominantly in either original biopanning experiments or in the following competitive binding assays. Sequences SB1, SB2 and SB3 showed a strongly increased binding efficiency compared to wild-type, at least 80fold higher, whereas SB4 showed a slightly higher affinity (~10 fold). Interestingly, SB4 was predominantly found in the competitive binding assay, an additional round of biopanning. These shifts in the peptide composition and motif frequency within phage libraries can be the result of the phage amplification in *E. coli*, which is necessary for further panning rounds. However, every amplification step introduces a library bias, as previously described [22,23]. Amplification

principles in bacteria differ from the biopanning selection pressure. Codon usage, amino acid preferences for bacterial infection, transport processes and protein folding strongly influence the composition of the phage library. Therefore amplification processes, although necessary, need to be minimized. High occurrence and relatively low binding properties occur most likely because of the previously discussed amplification bias, impressively illustrating the influence of only one additional amplification step. Bakhshinejad et al. demonstrated, that this loss-of-function may be the result of amplification advantages of fast-propagating phage over slow-propagating phage. Another explanation of the binding behavior and high abundance of SB4 may be, that adsorption to plastic surfaces [24] and albumin [25] cannot be prevented and may result in enrichment of phage with off-target binding affinities.

Immunofluorescence did show the superior binding behavior of chosen phage SB1. High fluorescence of antibody-marked phage could be measured on CAT material treated with SB1, with little to no fluorescence detection of CAT treated with wild-type phage (compare Fig. 3 A3, B3). Even after elution, detection of high fluorescence was still possible, because strongly bound phage could not be removed with chosen elution conditions. These findings indicate, that SB1 might be a "super-binder" showing very high and resistant affinity to the target material. Similar results were described by Lederer et al. [12].

For further characterization of the materials selectivity of identified peptide sequences, binding assays were performed with $CeMgAl_{11}O_{19}:Tb^{3+}$ (CAT), $Y_2O_3:Eu^{3+}$ (YOX), $BaMgAl_{10}O_{17}:Eu^{2+}$ (BAM), $LaPO_4:Ce^{3+},Tb^{3+}$ (LAP) and halophosphate (HP), materials typically found in fluorescent lamp powder. For SB1, binding affinities towards LAP and BAM were equally high compared to CAT, while SB2 and SB3 did show high selectivity towards CAT with binding efficiencies being around three times higher in comparison to the other tested materials. SB4 however did show highest affinity for BAM, indicating that the mineral samples, which were chosen for biopanning may have been contaminated with BAM. However, this may not necessarily be true, as characteristics of CAT and BAM show similarities. Inorganic materials as CAT and BAM possess a complex structure, which may interfere with phage binding resulting in difficult biopanning experiments with e.g. the false positive identification of off-target binding phage [26]. In conclusion, peptide motifs specifically binding CAT as well as motifs binding a broader range of REE-containing materials were identified, paving the way to biotechnological solutions for REE recovery.

Ion-binding peptides. Besides the characterization of solid REE-binding peptides, we present the identification of peptide sequences for binding of the heavy metal ions of nickel and

cobalt. Following the biopanning on planar sol-gel material with ion exchange capacity, 28 unique potentially cobalt-binding sequences were discovered. With a frequency of 28/63 MSTGLSS was the most abundant peptide sequence, followed by VPILEGT with 5/63. Four additional motifs were found with a frequency of 2/63. All discovered sequences consist of no to little numbers of aromatic amino acids. Different contents of hydrophobic, charged, polar and hydroxylic amino acids are found in the discovered motifs. Especially the high abundant sequences share a theoretical pI ~ 5. The lack of aromatic amino acids is in contradiction to the findings of Ueda et al., who described tryptophan (W), phenylalanine (F) and tyrosine (Y) to have high metal ion affinity because of their aromatic amino acid side chains. Additionally histidine (H) and cysteine (C) did show the highest affinity to metal ions, while both are rarely found in our results [27,28]. However, Ph.D.^{TM}-C7C phage libraries naturally include two cysteines, which form a disulfide bridge, flanking the peptide motifs and possibly interacting with metal ions. Especially for cysteine these findings arise from the fact, that unpaired cysteines do have negative effects on phage infection, hence unpaired cysteine-containing peptides cannot be found in the biopanning results as they add negative selection pressure to the containing peptides and may even not be present in the original library [29], even though it was described to interact with Cu(II) [30]. Cobalt(II), nickel(II) and copper(II) are also generally used for immobilization of histidine-containing peptides and proteins [31,32]. This explains why histidine is found in the identified peptide motifs, however quantity was lower than expected. When compared to the retention properties of individual amino acids on IDA-Cu(II) [33], strong binding amino acids histidine, tryptophan and phenylalanine were not found in excess amount in the identified motifs, however the strong binding amino acids glutamine, valine and leucine were routinely found. Tryptophan may therefore interfere with phage infection or phage protein amplification as Hansen et al. also described it to strongly bind to metal ions [34]. Differences in occurrence can of course be explained by different binding and elution conditions, which have a strong influence on retention and binding behavior [35]. Binding behavior of isolated phage was determined using the same conditions as used in biopanning. Binding efficiencies measured were found to be in a range of wild-type binding behavior to 18fold higher binding. Generally, motifs occurring with higher frequency showed an increased affinity towards nickel ions, however strongest binding motifs SMN06 and SMN12 were only found with a frequency of 01/29. These findings were discussed above and may the result of several amplification steps favoring fast-propagating phage of slow-propagating phage [36–38]. Comparing motifs, originally identified to bind to nickel for their cobalt binding efficiencies and vice versa, we found that

sequences were identified, which preferred nickel over cobalt, although being identified as cobalt-binders. Additionally sequences were found, which bind to both metal ions equally good and those, which prefer cobalt. Also sequences were found, that bind to both metals worse compared to wild-type phage. Reasons for this are explained above. Generally we expected the identified sequences to bind to both metals as they show similar properties. Still, we could identify motifs, which selectively prefer one specific metal ion, even with experimental setup not discriminating between both, as no negative biopanning was carried out to prevent selection of fast-propagating off-target peptide sequences. Adaption of biopanning setup could easily lead to selection of motifs with even higher specificity.

Conclusion. In this study we demonstrated for both solid materials as e.g. CAT mineral and for heavy metal ions, that Phage Surface Display technology with appropriate biopanning conditions is suitable to identify peptide motifs, which bind to their target materials with high affinity and selectivity. Especially target material selection is nearly unlimited, promising wide application areas. We therefore propose the general usability of Phage Surface Display in resource technologies, opening completely new fields for biotechnological advances. These approaches are superior to conventional resource recovery technology especially comparing their ecological impact as in contrast no solid waste is produced and no harmful chemicals need to be used [39]. However, further characterization is needed to quantify process conditions, reusability and scale-up possibilities. Furthermore, for economic reasons, production of peptides most likely needs to be done by heterologous expression, which we could demonstrate to be simple and successful [40]. However, heterologously expressed peptides need to be carefully quantified with regard to their binding behavior and economic usability, as this may differ from phage binding results. In summary, we successfully transferred Phage Surface Display, until now mostly used for medical applications, to resource recovery, putting a new competitor on the market.

Conflict of interest statement

The authors declare that there is no conflict of interest.

Acknowledgments.

The authors of this study would like to thank Falk Lehmann and Katrin Flemming, their support has greatly appreciated. Special thanks to Dr. Jamie Scott for the pVIII phage library LX-4 and to Dr. Ulrich Soltmann from GMBU e.V. for providing materials and support for sol-gel synthesis.

References.

[1] Brierley CL. How will biomining be applied in future? Trans Nonferrous Met Soc China 2008;18:1302–10. doi:10.1016/S1003-6326(09)60002-9.

[2] Bosecker K. Bioleaching: metal solubilization by microorganisms. FEMS Microbiol Rev 1997;20:591–604. doi:10.1016/S0168-6445(97)00036-3.

[3] Johnson DB. Development and application of biotechnologies in the metal mining industry. Environ Sci Pollut Res 2013;20:7768–76. doi:10.1007/s11356-013-1482-7.

[4] Johnson DB. Biomining—biotechnologies for extracting and recovering metals from ores and waste materials. Curr Opin Biotechnol 2014;30:24–31. doi:10.1016/j.copbio.2014.04.008.

[5] Vera M, Schippers A, Sand W. Progress in bioleaching: fundamentals and mechanisms of bacterial metal sulfide oxidation—part A. Appl Microbiol Biotechnol 2013;97:7529–41. doi:10.1007/s00253-013-4954-2.

[6] Sterritt RM, Lester JN. Interactions of heavy metals with bacteria. Sci Total Environ 1980;14:5–17. doi:10.1016/0048-9697(80)90122-9.

[7] Schrader S, Kutschke S, Rudolph M, Pollmann K. Production of Amphiphilic Hydroxamate Siderophores Marinobactins by <i>Marinobacter</i> sp. DS40M6 for Bioflotation Process. Solid State Phenom 2017;262:413–6. doi:10.4028/www.scientific.net/SSP.262.413.

[8] Kuzmicheva GA, Belyavskaya VA. Peptide phage display in biotechnology and biomedicine. Biochem (Moscow), Suppl Ser B Biomed Chem 2017;11:1–15. doi:10.1134/S1990750817010061.

[9] Seker UOS, Demir HV. Material Binding Peptides for Nanotechnology. Molecules 2011;16:1426–51. doi:10.3390/molecules16021426.

[10] Care A, Bergquist PL, Sunna A. Solid-binding peptides: smart tools for nanobiotechnology. Trends Biotechnol 2015;33:259–68. doi:10.1016/j.tibtech.2015.02.005.

[11] Bonnycastle LLC, Mehroke JS, Rashed M, Gong X, Scott JK. Probing the Basis of Antibody Reactivity with a Panel of Constrained Peptide Libraries Displayed by Filamentous Phage. J Mol Biol 1996;258:747–62. doi:10.1006/jmbi.1996.0284.

[12] Lederer FL, Curtis SB, Bachmann S, Dunbar WS, MacGillivray RTA. Identification of lanthanum-specific peptides for future recycling of rare earth elements from compact fluorescent lamps. Biotechnol Bioeng 2017;114:1016–24. doi:10.1002/bit.26240.

[13] Curtis SB, Hewitt J, MacGillivray RTA, Dunbar WS. Biomining with bacteriophage: Selectivity of displayed peptides for naturally occurring sphalerite and chalcopyrite. Biotechnol Bioeng 2009;102:644–50. doi:10.1002/bit.22073.

[14] Barbas CF. Phage display : a laboratory manual. Cold Spring Harbor Laboratory Press; 2001.

[15] Schönberger N, Matys S, Flemming K, Lehmann F, Lederer FL, Pollmann K. Development of Metal Ion Binding Peptides Using Phage Surface Display Technology. Solid State Phenom 2017;262:591–5. doi:10.4028/www.scientific.net/SSP.262.591.

[16] Ploss M, Facey SJ, Bruhn C, Zemel L, Hofmann K, Stark RW, et al. Selection of peptides binding to metallic borides by screening M13 phage display libraries. BMC Biotechnol 2014;14:12. doi:10.1186/1472-6750-14-12.

[17] Matys S, Lederer FL, Schönberger N, Braun R, Lehmann F, Flemming K, et al. Phage Display - A Promising Tool for the Recovery of Valuable Metals from Primary and Secondary Resources. Solid State Phenom 2017;262:443–6. doi:10.4028/www.scientific.net/SSP.262.443.

[18] Gasteiger E, Hoogland C, Gattiker A, Duvaud S, Wilkins MR, Appel RD, et al. Protein Identification and Analysis Tools on the ExPASy Server. Proteomics Protoc. Handb., Totowa, NJ: Humana Press; 2005, p. 571–607. doi:10.1385/1-59259-890-0:571.

[19] Hatanaka T, Matsugami A, Nonaka T, Takagi H, Hayashi F, Tani T, et al. Rationally designed mineralization for selective recovery of the rare earth elements. Nat Commun 2017;8:15670. doi:10.1038/ncomms15670.

[20] Chen H, Su X, Neoh K-G, Choe W-S. QCM-D Analysis of Binding Mechanism of Phage Particles Displaying a Constrained Heptapeptide with Specific Affinity to SiO 2 and TiO 2. Anal Chem 2006;78:4872–9. doi:10.1021/ac0603025.

[21] Chen C-L, Rosi NL. Peptide-Based Methods for the Preparation of Nanostructured Inorganic Materials. Angew Chemie Int Ed 2010;49:1924–42. doi:10.1002/anie.200903572.

[22] Derda R, Tang SKY, Li SC, Ng S, Matochko WL, Jafari MR. Diversity of Phage-Displayed Libraries of Peptides during Panning and Amplification. Molecules 2011;16:1776–803. doi:10.3390/molecules16021776.

[23] Rodi DJ, Soares AS, Makowski L. Quantitative Assessment of Peptide Sequence Diversity in M13 Combinatorial Peptide Phage Display Libraries. J Mol Biol 2002;322:1039–52. doi:10.1016/S0022-2836(02)00844-6.

[24] Menendez A, Scott JK. The nature of target-unrelated peptides recovered in the screening of phage-displayed random peptide libraries with antibodies. Anal Biochem 2005;336:145–57. doi:10.1016/j.ab.2004.09.048.

[25] Vodnik M, Zager U, Strukelj B, Lunder M. Phage Display: Selecting Straws Instead of a Needle from a Haystack. Molecules 2011;16:790–817. doi:10.3390/molecules16010790.

[26] Baneyx F, Schwartz DT. Selection and analysis of solid-binding peptides. Curr Opin Biotechnol 2007;18:312–7. doi:10.1016/j.copbio.2007.04.008.

[27] Ueda EK., Gout P., Morganti L. Current and prospective applications of metal ion–protein binding. J Chromatogr A 2003;988:1–23. doi:10.1016/S0021-9673(02)02057-5.

[28] DeSilva TM, Veglia G, Porcelli F, Prantner AM, Opella SJ. Selectivity in heavy metal-binding to peptides and proteins. Biopolymers 2002;64:189–97. doi:10.1002/bip.10149.

[29] McConnell SI, Uveges AJ, Fowlkes DM, Spinella DG. Construction and screening of M13 phage libraries displaying long random peptides. Mol Divers 1996;1:165–76. doi:10.1007/BF01544954.

[30] Kotrba P, Dolecková L, de Lorenzo V, Ruml T. Enhanced bioaccumulation of heavy metal ions by bacterial cells due to surface display of short metal binding peptides. Appl Environ Microbiol 1999;65:1092–8.

[31] Porath J, Olin B. Immobilized metal ion affinity adsorption and immobilized metal ion affinity chromatography of biomaterials. Serum protein affinities for gel-immobilized iron and nickel ions. Biochemistry 1983;22:1621–30.

[32] Vançan S, Miranda EA, Bueno SMA. IMAC of human IgG: studies with IDA-immobilized copper, nickel, zinc, and cobalt ions and different buffer systems. Process

Biochem 2002;37:573–9. doi:10.1016/S0032-9592(01)00242-4.

[33] Yip T-T, Nakagawa Y, Porath J. Evaluation of the interaction of peptides with Cu(II), Ni(II), and Zn(II) by high-performance immobilized metal ion affinity chromatography. Anal Biochem 1989;183:159–71. doi:10.1016/0003-2697(89)90184-X.

[34] Hansen P, Lindeberg G. Purification of tryptophan containing synthetic peptides by selective binding of the α-amino group to immobilised metal ions. J Chromatogr A 1994;662:235–41. doi:10.1016/0021-9673(94)80510-5.

[35] Shiba K. Natural and artificial peptide motifs: their origins and the application of motif-programming. Chem Soc Rev 2010;39. doi:10.1039/b719081f.

[36] Rentero Rebollo I, Sabisz M, Baeriswyl V, Heinis C. Identification of target-binding peptide motifs by high-throughput sequencing of phage-selected peptides. Nucleic Acids Res 2014;42:e169. doi:10.1093/nar/gku940.

[37] Zanconato S, Minervini G, Poli I, De Lucrezia D. Selection dynamic of Escherichia coli host in M13 combinatorial peptide phage display libraries. Biosci Biotechnol Biochem 2011;75:812–5. doi:10.1271/bbb.110099.

[38] He B, Tjhung KF, Bennett NJ, Chou Y, Rau A, Huang J, et al. Compositional Bias in Naïve and Chemically-modified Phage-Displayed Libraries uncovered by Paired-end Deep Sequencing. Sci Rep 2018;8:1214. doi:10.1038/s41598-018-19439-2.

[39] Binnemans K, Jones PT, Blanpain B, Gerven T Van, Yang Y, Walton A, et al. Recycling of rare earths: a critical review. J Clean Prod 2013;51:1–22. doi:10.1016/j.jclepro.2012.12.037.

[40] Braun R, Matys S, Schönberger N, Lederer FL, Pollmann K. Simplified Expression and Production of Small Metal Binding Peptides. Solid State Phenom 2017;262:447–51. doi:10.4028/www.scientific.net/SSP.262.447.

Tables

Table 1: Summary of the occurrences of the selected, identified peptide sequences and their general amino acid composition. R arginine, H histidine, K lysine, D aspartic acid, E glutamic acid, S serine, T threonine, N asparagine, Q glutamine, C cysteine, G glycine, P proline, A alanine, I isoleucine, L leucine, M methionine, F phenylalanine, W tryptophan, Y tyrosine, V valine.

sequence motif		normalized binding efficiency	relative occurrence / frequenvy	competitive occurrence	theoretical pI	hydrophilic	hydrophobic	acidic	basic
KKQKCRTDACVTQM	SB1	128.6 ± 23.5	07/80	01/30	9.39	11	3	1	4
NEKKCKGARCTTVT	SB2	84.3 ± 19.4	03/80	03/30	9.39	11	2	1	4
ATPKCKKKSCMTTQ	SB3	94.5 ± 29.9	03/80	08/30	9.70	11	2	0	4
VDKKCKSDDCGAWH			03/80	00/30	6.70	10	3	3	4
HDKKCKRQPCVLAN			02/80	01/30	9.39	10	3	1	5
FDKKCKSNKCLEVR			02/80	01/30	9.31	11	3	2	6
PKKKCHPEPCQTCG			02/80	01/30	8.77	10	0	1	4
KTEHCKKRKCPLDM			02/80	01/30	9.31	11	2	2	6
ETKKCTTGPCKVVT	SB4	13.4 ± 4.7	02/80	14/30	8.87	10	2	1	3
KKKKCKKKICTTHT			01/80	00/30	10.16	13	1	0	8
KKKKCKKNTCKNHT			01/80	00/30	10.16	14	0	0	8

Table 2: Occurrence, general amino acid composition and theoretical pI (calculated with Expasy ProtParam) of selected, identified cobalt (A) and nickel (B) binding peptide sequences using Phage Surface Display.

sequence motif		relative occurrence / frequency	normalized binding efficiency	theoretical pI	hydrophobic	charged	polar	aromatic	hydroxylic
A			**Cobalt-binding peptide motifs**						
MSTGLSS	SMC01	28 / 63	2.8 ± 0.7	5.28	3	0	4	0	4
VPILEGT	SMC02	05 / 63	1.5 ± 0.3	4.00	5	1	1	0	1
DRTISNK	SMC03	02 / 63	1.8 ± 0.5	8.75	2	3	3	0	2
QNPGNTL	SMC04	02 / 63	2.5 ± 0.9	5.52	3	0	4	0	1
SGTGASY	SMC05	02 / 63	1.7 ± 0.7	5.24	2	0	3	1	3
SSSVVTH	SMC06	02 / 63	2.3 ± 0.9	6.46	3	1	4	0	4
DAKDLNS	SMC07	01 / 63	2.5 ± 0.9	4.21	2	3	2	0	1
DNDTKAS	SMC08	01 / 63	1.5 ± 0.5	4.21	2	3	3	0	2
GLTDTSN	SMC09	01 / 63	0.8 ± 0.3	3.80	3	1	4	0	3
KTSTHAI	SMC10	01 / 63	1.5 ± 0.3	8.76	4	2	3	0	3
MRDSKML	SMC11	01 / 63	2.2 ± 0.6	8.50	3	3	1	0	1
STISKAK	SMC12	01 / 63	2.6 ± 0.8	10.00	3	2	3	0	3
TASQNFY	SMC13	01 / 63	1.4 ± 0.2	5.18	2	0	4	2	2
TGQGGEY	SMC14	01 / 63	1.5 ± 0.2	4.00	1	1	2	1	1
TKTQTHA	SMC15	01 / 63	0.8 ± 0.0	8.44	4	2	4	0	3
TNHSAYH	SMC16	01 / 63	2.7 ± 2.0	6.61	2	2	3	1	2
TQMLGQL	SMC17	01 / 63	1.4 ± 0.27	5.19	4	0	3	0	1
VSPNKEA	SMC18	01 / 63	3.1 ± 0.7	5.97	3	2	2	0	1
B			**Nickel-binding peptide motifs**						
SGTGASY	SMN01	03 / 29	5.9 ± 1.7	5.24	2	0	3	1	3
MSTGLSS	SMN02	02 / 29	4.0 ± 2.9	5.28	3	0	4	0	4
NTGSPYE	SMN03	02 / 29	1.2 ± 0.0	4.00	2	1	3	1	2
TASQNFY	SMN04	02 / 29	10.4 ± 0.0	5.18	2	0	4	2	2
GSRSAQT	SMN05	01 / 29	2.0 ± 1.1	9.75	2	1	4	0	3
GTKGSLN	SMN06	01 / 29	17.8 ± 3.0	8.75	2	1	3	0	2
GYSSFNR	SMN07	01 / 29	3.6 ± 1.2	8.75	0	1	3	2	2
HHPVANT	SMN08	01 / 29	1.1 ± 0.2	6.92	4	2	2	0	1
HNETQKM	SMN09	01 / 29	1.6 ± 0.6	6.75	2	3	3	0	1
KDTSRSA	SMN10	01 / 29	1.2 ± 0.1	8.75	2	3	3	0	3
NAKHHPR	SMN11	01 / 29	16.8 ± 6.5	11.00	2	4	1	0	0
NGRAVNY	SMN12	01 / 29	0.9 ± 0.5	8.75	2	1	2	1	0
PGASVTY	SMN13	01 / 29	1.1 ± 1.0	5.95	4	0	2	1	2
RAEGTSE	SMN14	01 / 29	1.0 ± 0.0	4.53	2	3	2	0	2
RGATPMS	SMN15	01 / 29	1.0 ± 0.7	9.75	4	1	2	0	2
SLATDQK	SMN16	01 / 29	2.1 ± 0.8	5.55	3	2	3	0	2
SNNHSSM	SMN17	01 / 29	2.2 ± 1.0	6.46	1	1	5	0	3
STATPYK	SMN18	01 / 29	2.4 ± 1.5	8.31	4	1	3	1	3
TKTDVHF	SMN19	01 / 29	2.6 ± 2.0	6.41	3	3	2	1	2
TSVLNNT	SMN20	01 / 29	2.4 ± 0.4	5.19	4	0	5	0	3
VPILEGT	SMN21	01 / 29	1.9 ± 0.8	4.00	5	1	1	0	1

Figures

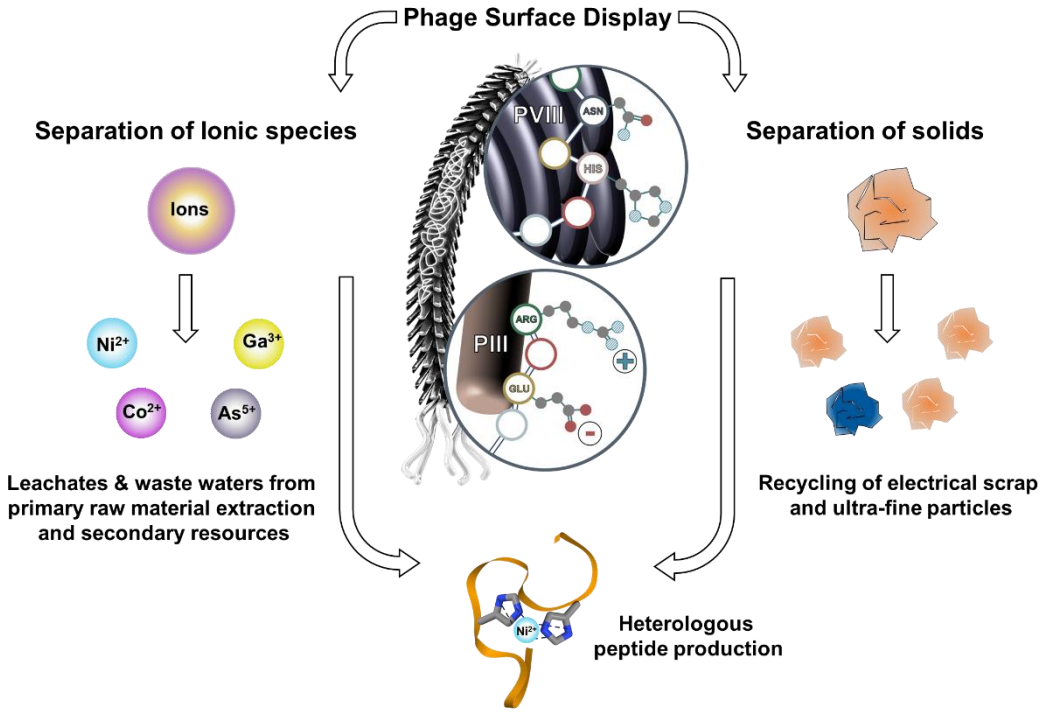

Fig. 1: Scheme of Phage Surface Display usage for biomining approaches. Peptides are used for separation of ionic species (left) and solids (right) and may be further optimized using genetic engineering for efficient heterologous production.

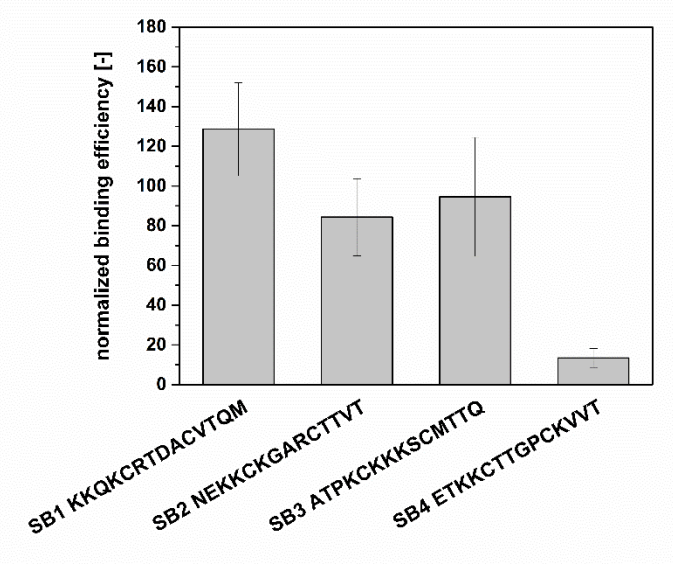

Fig. 2: Normalized results of the binding assays performed with CAT minerals and phage displaying the shown amino acid sequences. Binding efficiency was calculated by determining phage titer before and after binding and elution for selected phage. Results are normalized against wild-type phage.

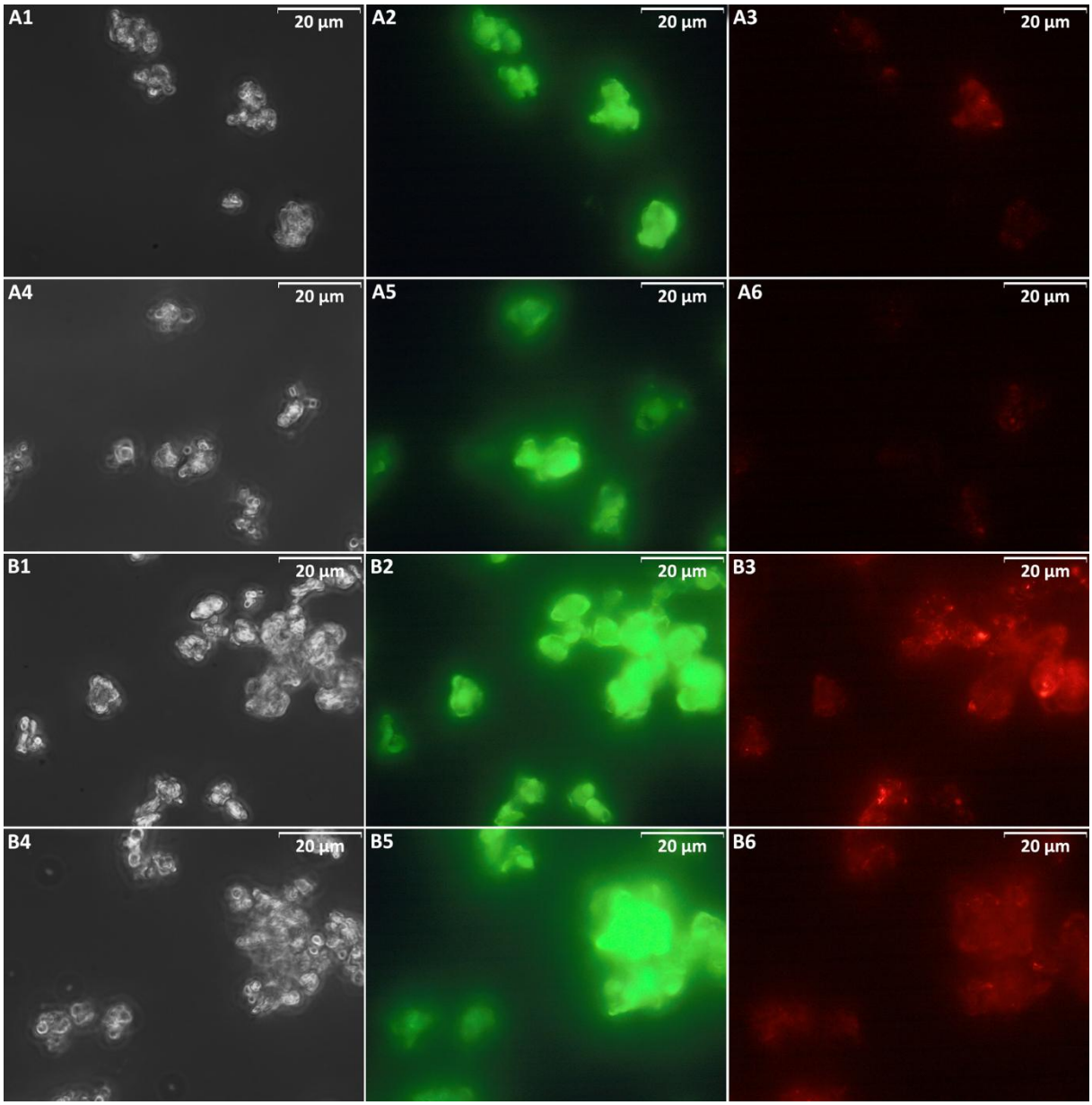

Fig. 3: Phase contrast (1,4) and fluorescence microscopy pictures (filter U-MNU 2, 5 and filter U-N39010 3,6) of phage displaying the sequence SB1 KKQKCRTDACVTQM (B) and wild-type phage (A) to CAT mineral. Pictures were taken after phage binding and antibody marking before elution of phage (1-3) and after elution of phage with elution buffer (4 – 6).

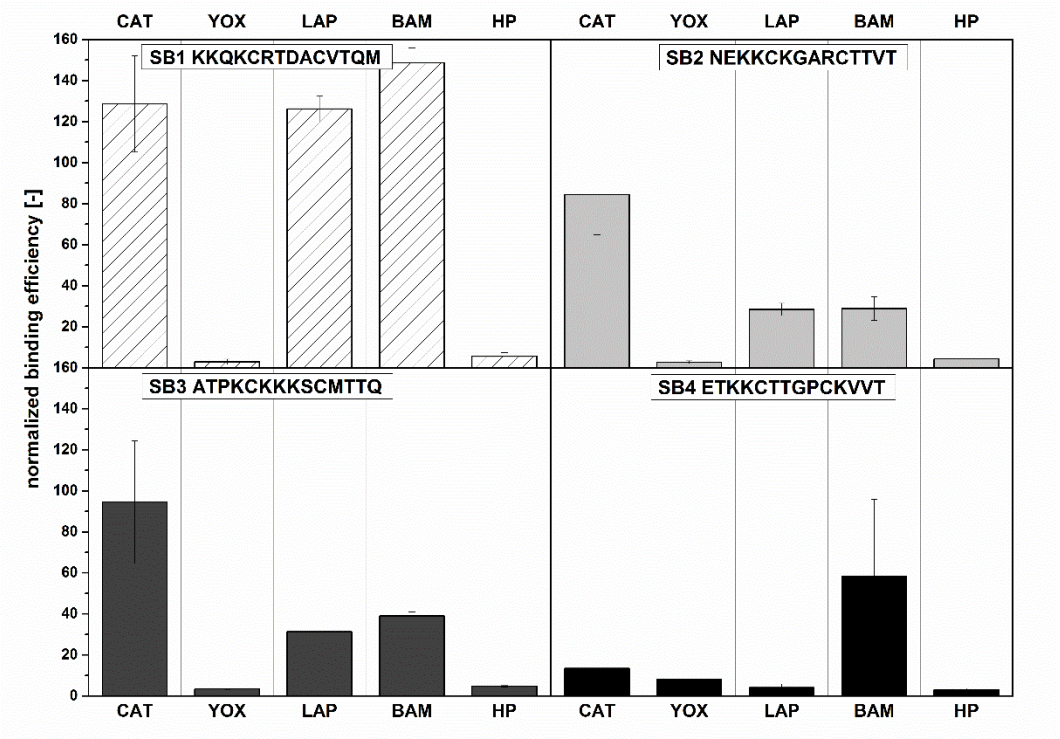

Fig. 4: Comparison of the binding efficiencies of four selected phage to different materials, which are part of fluorescent lamp powder. Binding efficiency was calculated by determining phage titer before and after binding and elution for selected phage normalized against wild-type phage. Materials tested were $CeMgAl_{11}O_{19}:Tb^{3+}$ (CAT), $Y_2O_3:Eu^{3+}$ (YOX), $BaMgAl_{10}O_{17}:Eu^{2+}$ (BAM), LaPO4:Ce,Tb (LAP) and halophosphate (HP).

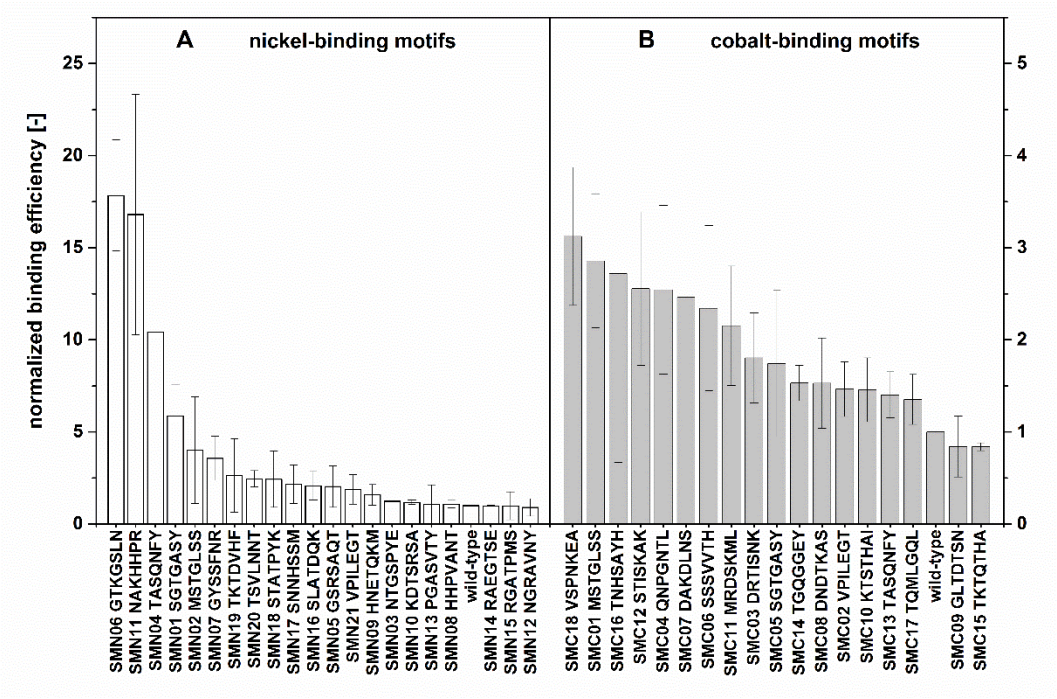

Fig. 5: Normalized binding efficiencies of identified peptide motifs determined in comparison of phage titer before and after binding and elution for selected phage normalized against wild-type phage for nickel-binding sequences (A) and cobalt-binding sequences (B).

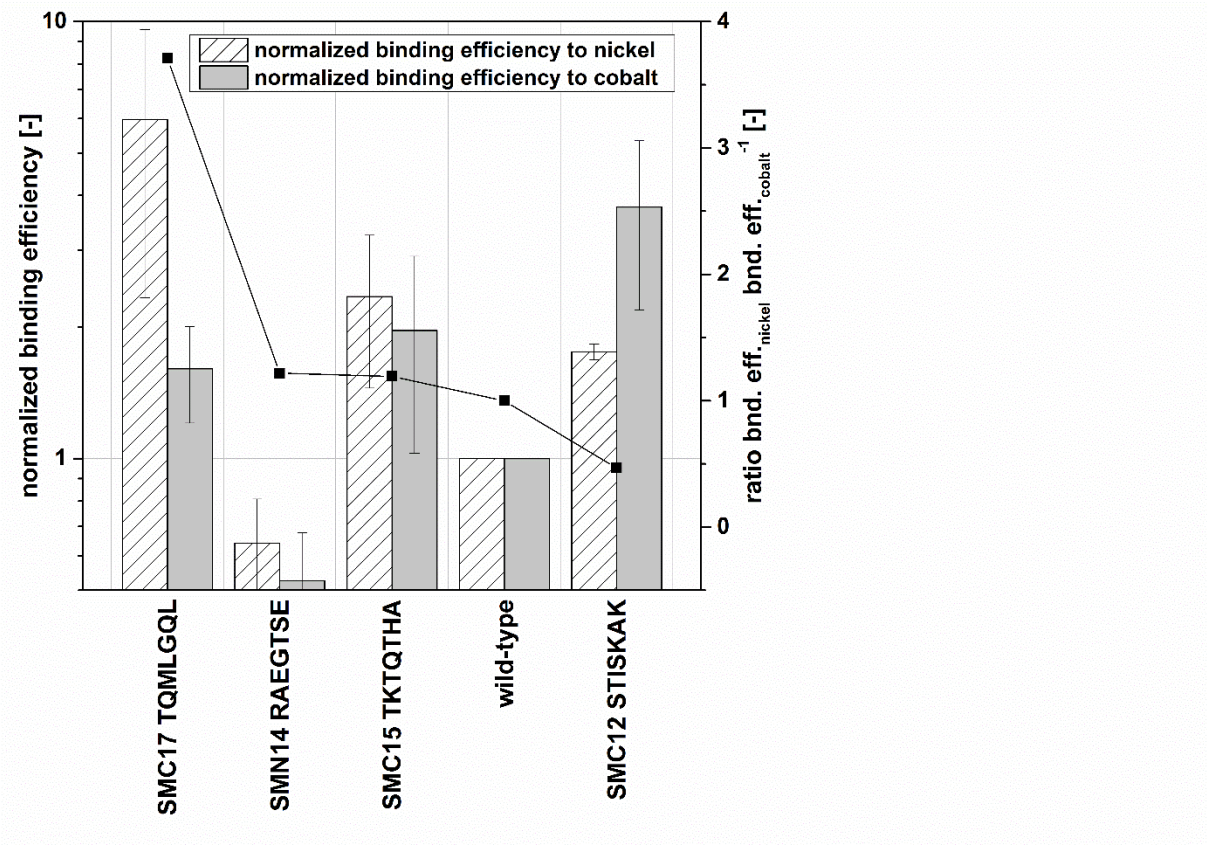

Fig. 6: Cross-binding of selected peptide motifs. Sequences found in nickel biopanning were characterized for their binding efficiency towards cobalt and vice versa. Binding efficiencies were determined as ratio of phage titer in input and eluate fractions of binding assays and were normalized against the wild-type phage binding behavior. For comparison of nickel- and cobalt-binding, the ratio of both binding efficiencies is shown.

Fig1

Click here to download high resolution image

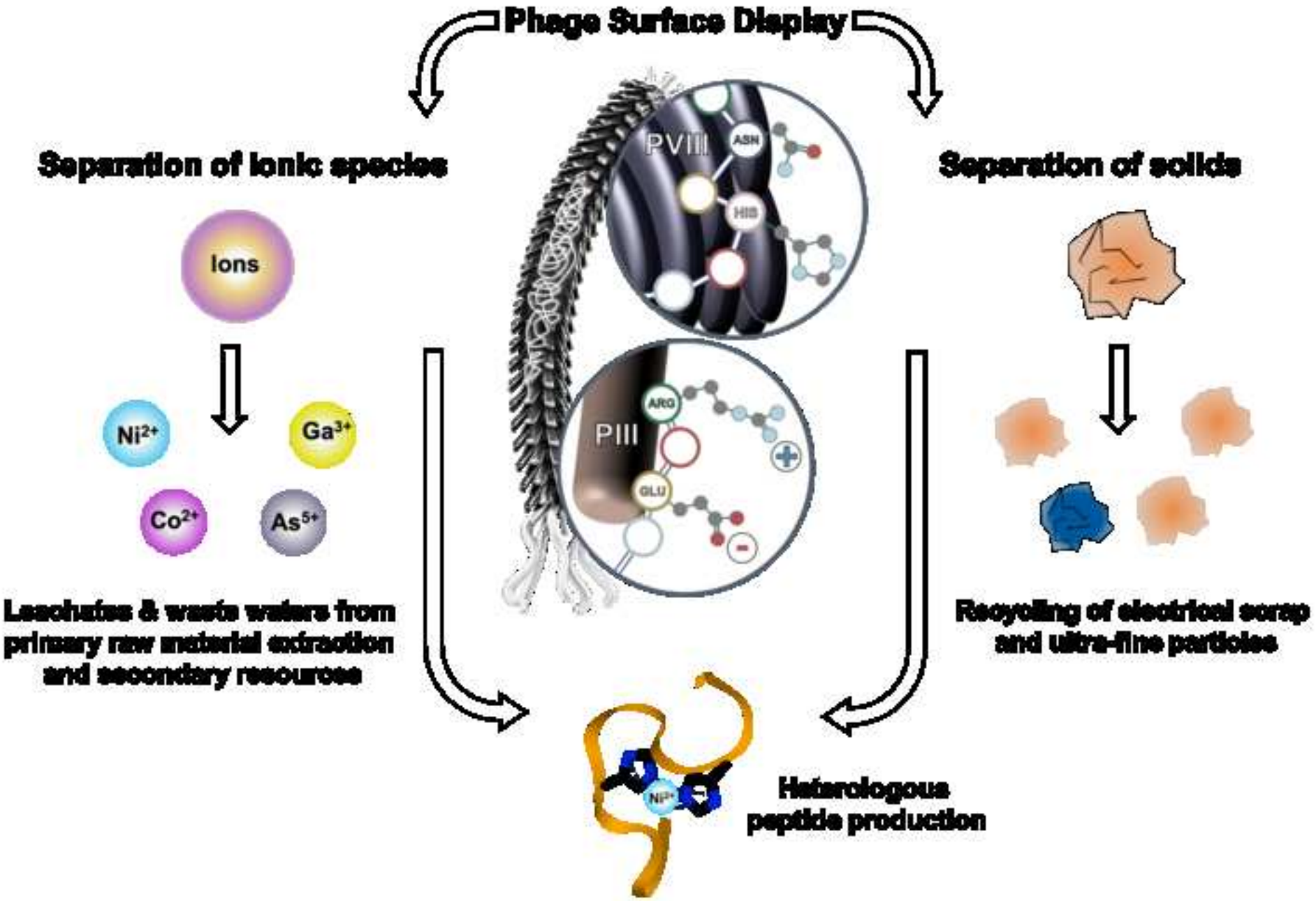

Fig2

Click here to download high resolution image

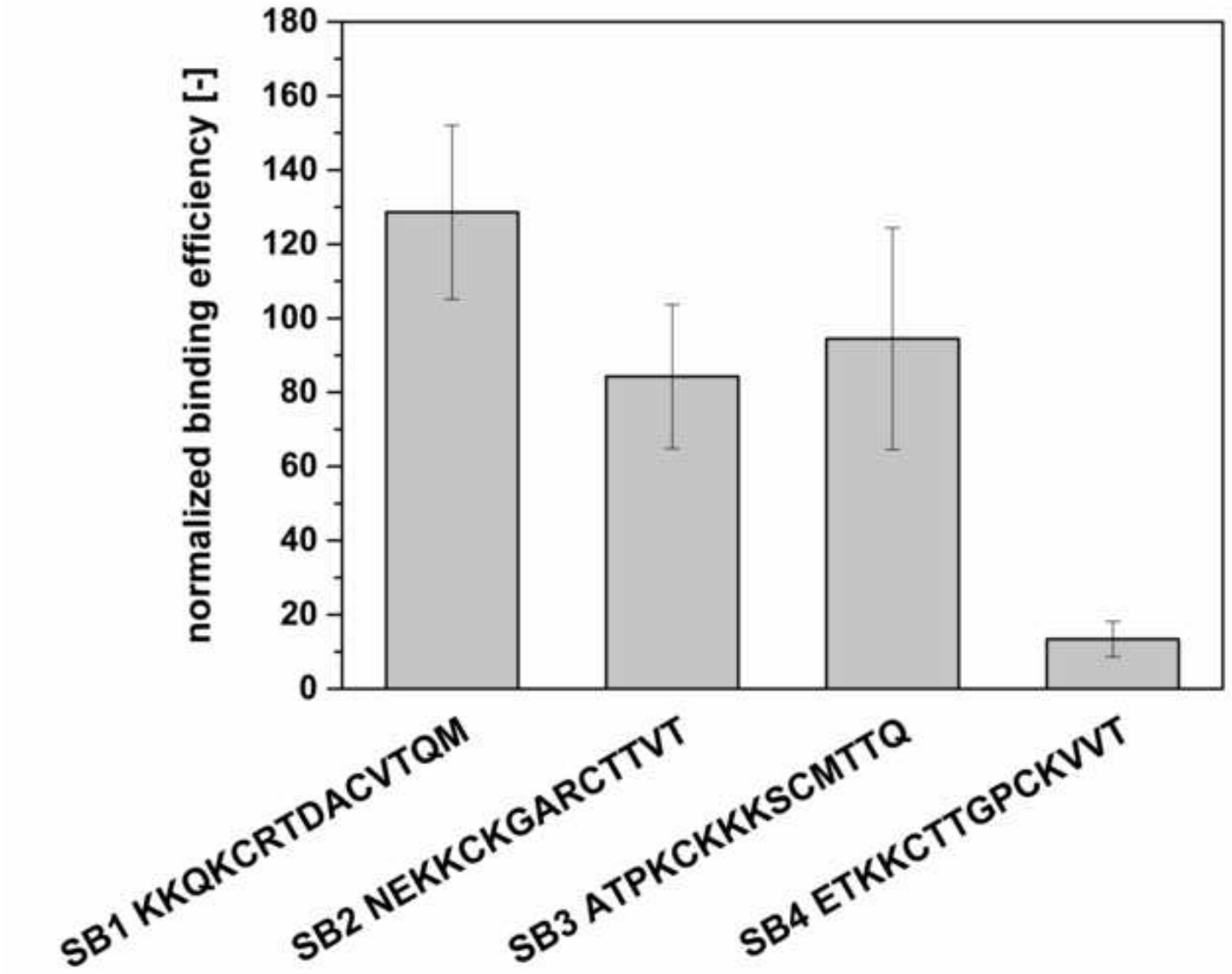

Fig3

Click here to download high resolution image

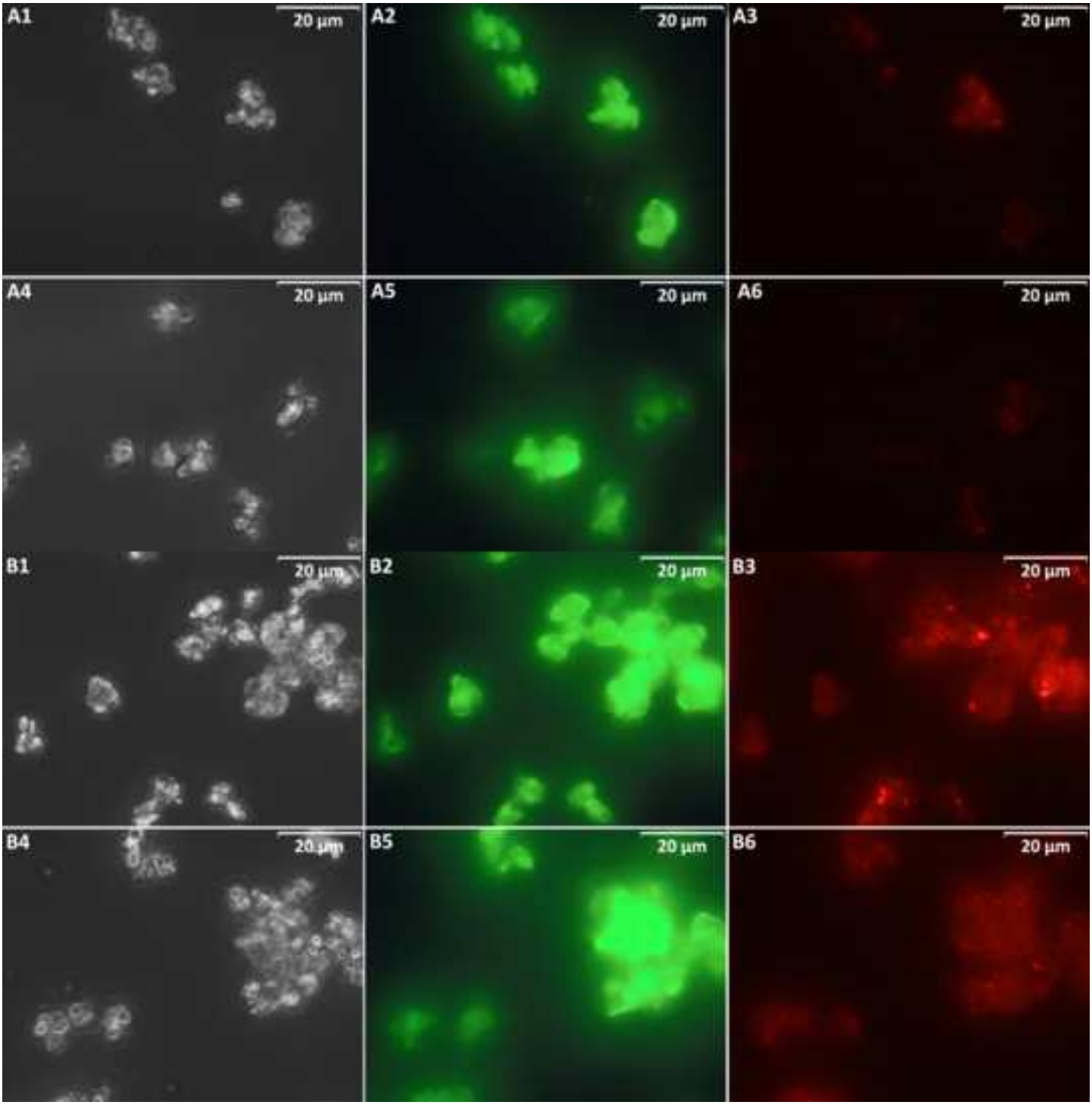

Fig4

Click here to download high resolution image

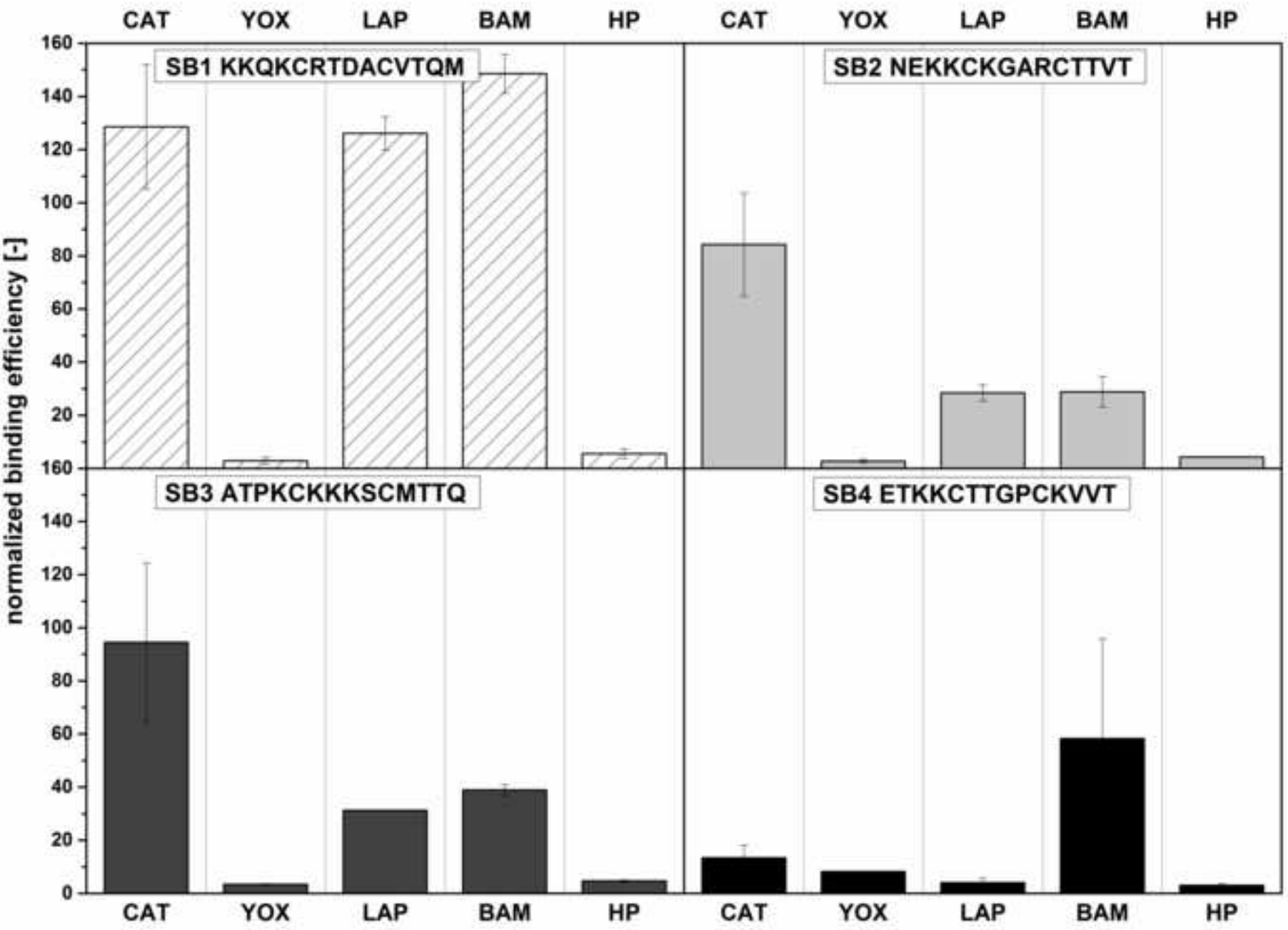

Fig5

Click here to download high resolution image

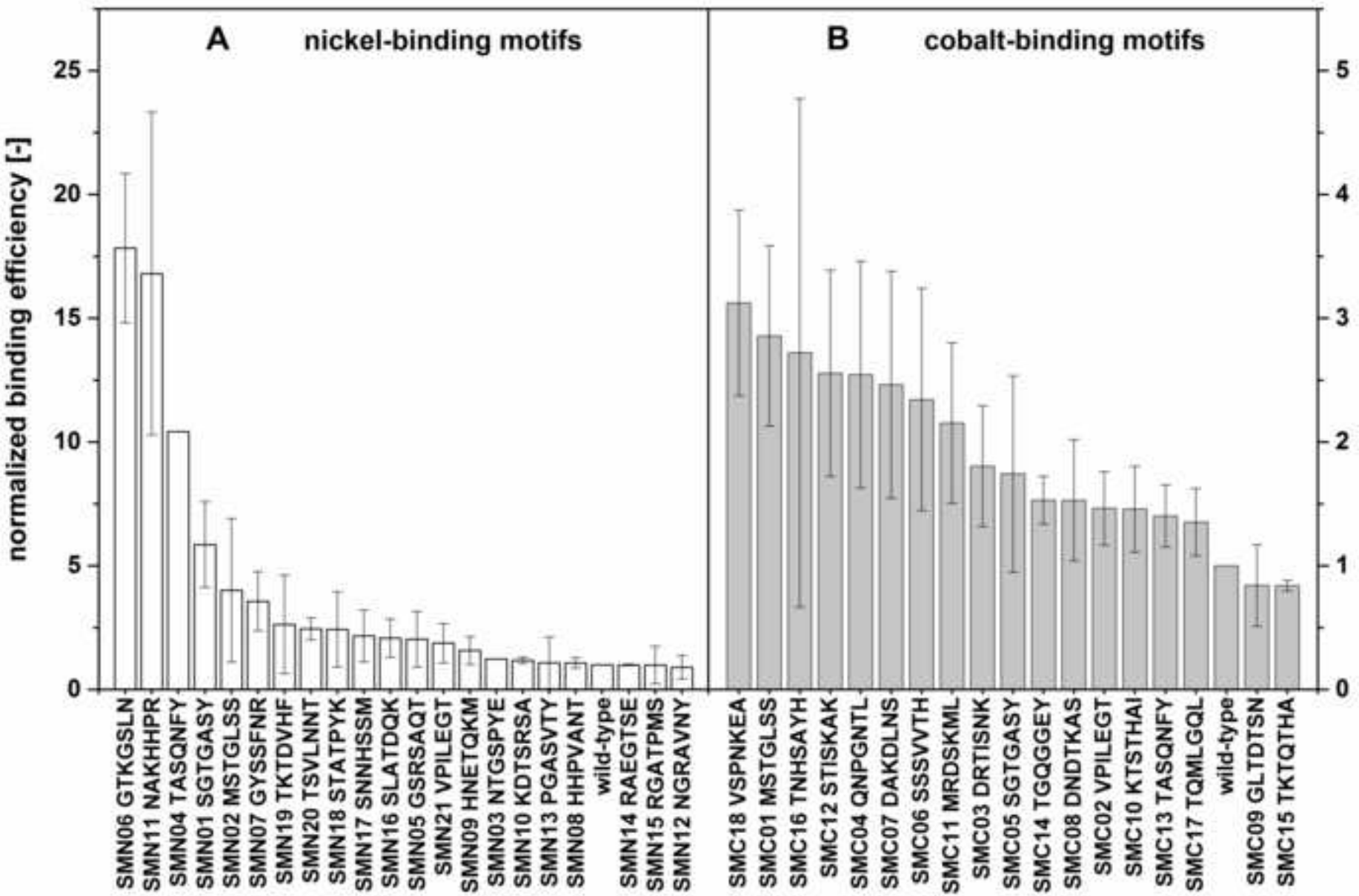

Fig6

Click here to download high resolution image